Early role for IL6 signaling in iPS generation revealed by heterokaryon RNA-Seq

Jennifer J. Brady[1], **Mavis Li**[2,3], **Silpa Suthram**[1], **Hui Jiang**[2,3,4], **Wing H. Wong**[3], and **Helen M. Blau**[1,5]

[1]Baxter Laboratory for Stem Cell Biology, Department of Microbiology and Immunology, Institute for Stem Cell Biology and Regenerative Medicine, Stanford University School of Medicine, Stanford, California 94305, USA

[2]Institute for Computational and Mathematical Engineering, Stanford University, Stanford, California 94305, USA

[3]Department of Statistics, Stanford University, Stanford, California 94305, USA

Molecular insights into somatic cell reprogramming to iPS would aid regenerative medicine, but are difficult to elucidate in iPS because of their heterogeneity, as relatively few undergo reprogramming (0.1-1%)[1,2]. To identify early acting regulators, we capitalized on non-dividing heterokaryons (mouse embryonic stem cells (mES) fused to human fibroblasts (hFb)), in which reprogramming towards pluripotency is efficient and rapid[3], enabling the identification of transient regulators required at the onset. We used bi-species transcriptome-wide RNA-Seq to quantitate transcriptional changes in the human somatic nucleus during reprogramming toward pluripotency in heterokaryons. During heterokaryon reprogramming, the cytokine interleukin 6 (*IL6*), which is not detectable at significant levels in ES cells, was induced 50-fold. A 4-day culture with IL6 at the onset of iPS reprogramming replaced stably transduced oncogenic c-Myc such that transduction of only Oct4, Klf4, and Sox2 was required. IL6 also activated another Jak-Stat target, the serine-threonine kinase *Pim1*, which accounted for the IL6-mediated 2-fold increase in iPS frequency. By contrast, LIF, another induced GP130 ligand, failed to increase iPSor activate *c-Myc* or *Pim1*, thereby revealing a differential role for the two Jak-Stat inducers in iPS generation. These findings demonstrate the power of heterokaryon bi-species global RNA-Seq to identify early acting regulators of reprogramming, for example extrinsic replacements for stably transduced transcription factors such as the potent oncogene c-Myc.

[5]Correspondence should be addressed to H.M.B.: Helen M. Blau, 269 Campus Drive, Stanford, California 94305-5175, USA, Tel: 650-723-6209, Fax: 650-736-0080, hblau2@stanford.edu.
[4]Present Address: Department of Biostatistics, University of Michigan, Ann Arbor, Michigan 48109, USA

Heterokaryons are ideally suited to elucidating regulators at the onset of reprogramming. When fused to human fibroblasts, mouse embryonic stem cells provide a panoply of stem cell factors in abundance, as the ratio is skewed to favor mouse ES cells leading toa rapid induction of pluripotency transcriptsin the somatic human fibroblast that can be distinguished based on species differences[3]. To identify previously unrecognized early acting regulators of reprogramming, we monitored heterokaryon gene expression over a 3-day time course during which no cell division occurs[3]. Heterokaryons generated from an excess of mouse GFP^{+} ES cells and DsRed[+] human fibroblasts were enriched to 80% purity by FACS (Fig. 1a, b). The nuclear ratio (mouse: human) was determined by the relative abundance of mouse Dppa5 promoter copy number relative to human OCT4 promoter copy number by genomic qPCR, revealing an average nuclear ratio of 3.4 ± 0.3 mouse nuclei to 1 human nucleus (mean $\pm$ s.d.). In good agreement, FACS sorted heterokaryons analyzed singly by microscopy were found to have a mean content of 4 nuclei, when fitted to a Gaussian distribution (Fig. 1c).

Following heterokaryon isolation by FACS and Illumina library construction, sequencing revealed that the average heterokaryon RNA-Seq library yielded 15.5 million reads which had an 87% mappable rate when aligned to mouse and human genomes ($\sim$23,400 genes for mouse and $\sim$40,000 genes for human; see Table SI 1). In accordance with the nuclear ratio, the mappable reads consisted of 70% mouse, 26% human, and 4% that were common to both species (Fig. 1d, workflow outlined in Fig. 1e). Of the total mappable reads, 4% were eliminated due to species homology. However, importantly, no coding gene was entirely eliminated from the analysis. In order to quantify gene expression for transcripts with significant conservation between the mouse and human transcriptomes, we modified the original definition of RPKM (Reads Per Kilobase of exon model per Million mappable reads, the standard measure of gene expression using RNA-Seq)[4] to account for the length of the conserved regions (see Supplementary Note 1). Heterokaryon human RPKM values showed a high level of reproducibility across biological replicates for days 1, 2 and 3, with Pearson correlation values of >0.95 (Fig. 1f). To focus our analysis on reprogramming specific to the somatic cell nucleus, we compared human gene expression over the heterokaryon timecourse with three control populations: human fibroblasts alone (hFb), fused fibroblast homokaryons (homok), and unfused co-cultures of fibroblasts and mES cells (co-cult). Hierarchical clustering of all of the samples showed that gene expression over the three days was closer in heterokaryon samples compared to the controls, highlighting the quality of the data generated (Fig. 1g).

We identified a total of 905 differentially expressed genes over the three days using the NOISeq method analytic package[5], as shown in the Venn diagrams (Fig. 1h, 1i, and Table SI 1). NOISeq analysis of heterokaryon reprogramming revealed 630 up-regulated and 275 down-regulated human genes unique to reprogramming (Fig. 2a and Table SI 1). These genes separated into 28 PANTHER protein classes with transcription factors, nucleic acid binders, signaling molecules, and receptors comprising 34% of the differentially expressed genes (Fig. 2b and Table SI 1)[6]. Several of the expected pluripotency transcription factors were induced in human fibroblasts (Fig. 2c). Additionally, we observed the induction of GP130 signaling pathway genes, including the transcription factor *MYC*, the pro-survival

kinases *PIM1* and *PIM2*, the negative feedback regulator *SOCS3*, the anti-apoptotic BCL2 family member *MCL1*[7-9] and the GP130 ligands *LIF* and *IL6* (Fig. 2d), with *MYC*, *PIM1*, and *IL6* identified as significantly differentially expressed in the NOISeq analysis. The GP130-STAT3 responsive gene subset was induced in heterokaryons concomitantly with the majority of the human ES gene signature, as defined by others[10-12]. The fold inductions observed by RNA-Seq were comparable to those obtained by heterokaryon qPCR, validating the approach (Fig. 2e). Based on these findings, we postulated that IL6 plays a role in iPS reprogramming.

To determine whether IL6 or other IL6-type cytokine family members could be responsible for induction of the GP130 gene signature in heterokaryons, we examined the expression of the entire family of IL6 type cytokines, which consists of *IL6*, *LIF* (leukemia inhibitory factor), *OSM* (oncostatin M), *IL11* (interleukin-11), *CNTF* (ciliary neurotrophic factor), and *CT-1* (cardiotrophin-1)[8]. The transcript levels in the human RNA-Seq dataset identified *IL6* as the prime candidate, as it was the most highly induced, increasing by 50-fold on day 3 relative to unfused fibroblasts (Fig. 3a and Supplementary Fig. 1a). The only family member other than IL6 that exhibited >2-fold induction was *LIF*, which was induced 4-fold by day 3, suggesting these two cytokines as potential inducers of the GP130 signature gene expression seen in heterokaryons (Fig. 2d and 3a).

To determine whether in iPS generation, like heterokaryons, Il6 and Lif transcript levels were also induced, we examined their relative mRNA levels after 4F (OKSM) transduction of mouse embryonic fibroblasts (MEFs), cultured in the absence of exogenous cytokines. Both were expressed at low levels prior to fusion. However, *Il6*, but not *Lif*, was induced >2-fold by day 4 of iPS reprogramming (Fig. 3b). In addition, we found that the Il6 receptor (*Il6r*) was induced 6.6-fold during 4F reprogramming while the levels of Lif receptor (*Lifr*) did not exceed 1.4-fold induction (Supplementary Fig. 1b). In order to ensure the MEFs used for reprogramming were responsive to IL6 treatment, we tested whether exposure of MEFs to IL6 induced the Jak-Stat signal transduction pathway by assaying for phosphorylation of Stat3 Tyrosine (Tyr) 705[8]. Il6r receptor function was validated by detection of Stat3 Tyr-705 phosphorylation by western blot (Fig. 3c). Fibroblasts treated with IL6 resulted in significantly higher levels of pStat3 than unphosphorylated Stat3 relative to α-tubulin, peaking 30 minutes post-stimulation (Fig. 3d). Thus, *Il6* but not *Lif* was deemed the most likely candidate capable of enhancing iPS reprogramming via gp130.

To determine whether IL6 played a functional role in reprogramming somatic cells to iPS, the potential of IL6 to augment MEF reprogramming to iPS was investigated in combination with lentiviral transduction of 4F (Fig. 3e). iPS colonies were assessed by immunostaining for the pluripotency markers Nanog and SSEA-1 (Fig. 3f, g and Supplementary Fig. 2a, b). Inclusion of LIF had no effect above 4F on iPS colony yield, eliminating this cytokine as an enhancer of reprogramming to iPS (Fig. 3h). By contrast, IL6addition to the medium resulted in a 2.2 ± 0.2-fold increase in mouse iPS colony yield (mean ± s.e.m., n=3).

Because IL6-mediated Jak-Stat signaling is known to induce c-Myc, we tested whether transient extrinsic IL6 could replace stably integrated oncogenic viral c-Myc, which is frequently associated with human cancers and is one of the four transduced factors routinely

used to generate iPS. This possibility was also suggested by the heterokaryon NOISeq analysis, which revealed induction of *MYC* among the GP130 signature genes (Fig. 2d). To determine if IL6 induces endogenous *c-Myc* expression, we treated MEFs with IL6 and assessed c-Myc transcript levels by qPCR. We detected a 3.1 ± 0.7-fold induction of endogenous *c-Myc* transcripts (mean $\pm$ s.e.m., n=3), which peaked at 60 minutes post IL6 stimulation (Fig. 4a). Importantly, control MEFs treated with LIF, or medium change alone (mock) did not induce significant changes in *c-Myc* expression, demonstrating that the observed gene induction was specific to IL6 addition (Fig. 4a). To test whether IL6 could replace viral c-Myc, we generated a three-factor lentivirus containing Oct4, Klf4, and Sox2 (OKS, 3F) and a second virus encoding only c-Myc for direct comparison of 3F reprogramming with and without exogenous c-Myc (Fig. 4b). At day 12 post 3F transduction, no colonies were obtained for 3F only, or 3F + Mock virus. Notably, daily addition of IL6 to the reprogramming medium after transduction with 3F virus resulted in generation of Nanog$^+$ colonies, to levels comparable to the 3F + c-Myc control (Fig. 4c). These results show that addition of IL6 to the medium can replace the requirement for stable integration of the oncogene c-Myc.

As c-Myc is known to function early during iPS reprogramming[13], we postulated that IL6might also play an early role. To explore this hypothesis, we assessed the minimum time-window required for IL6 exposure in order to achieve maximum colony yield. Addition of IL6 to 3F transduced MEFs sufficed to achieve maximal iPS colony yield when added to the medium daily during the first four days of reprogramming and no increase in yield was seen if daily exposure to IL6 continued beyond this time point (Fig. 4d and Table SI 1). Hence, IL6 stimulation is necessary only transiently during an early time-window at the onset of reprogramming. Exogenous addition of IL6 to MEF cultures is dispensable 4 days post viral transduction for iPS generation and subsequent iPS maintenance. These results establish IL6 as an early regulator of iPS generation that does not require stable integration and acts transiently via addition to the media.

In order to characterize the pluripotency quality of IL6 + 3F-derived iPS clones, we first determined whether they expressed a similar panel of mouse ES pluripotency genes[14,15]. All 15 genes analyzed by RT-PCR were expressed in IL6 + 3F-derived iPS clones, 4F-derived iPS clones, and mouse ES, but not expressed in MEF controls (Supplementary Fig. 2c). IL6 + 3F-derived iPS clones were confirmed to be free of exogenous viral c-Myc integration using genomic PCR (Supplementary Fig. 2d). A more rigorous test of pluripotent potential entailed an *in vivo* analysis of the 3F + IL6-derived iPS clones by standard teratoma derivation. Staining and histological analyses of the resulting teratomas confirmed that IL6 + 3F-derived iPS clones could generate tissues representing all three germ layers (Fig. 4e). Global transcriptome analyses of 3F + IL6 iPS clones, 4F iPS clones, and mES confirmed these observations, as gene expression of all iPS clones (with and without transduced c-Myc) clustered closely with mES (Pearson correlation r=0.96) (Fig. 4f). Together, these results demonstrate that the pluripotent potential of 3F + IL6-derived iPS clones is comparable to that of 4F iPS.

The demonstration that IL6 could augment reprogramming efficiency 2.2-fold in the presence of the 4F where c-Myc levels are in excess (Fig. 3h) suggested that IL6 has

functional roles in addition to c-Myc induction that lead to enhanced iPS generation. Therefore, we explored the role of the pro-survival kinase Pim1, an additional downstream target of IL6-mediated GP130 signaling identified as significantly up-regulated in heterokaryons (Fig. 2d). *Pim1* was induced 3.4 ± 0.5-fold in MEFs (mean ± s.e.m., n=3), peaking at 90 minutes post-IL6 stimulation (Fig 5a). As with *c-Myc*, induction of *Pim1* was specific to IL6 stimulation and was not observed in LIF or mock treated MEFs. The role of Pim1 activity in IL6-mediated reprogramming was assessed by loss of function using two distinct and highly specific Pim1 inhibitors[16, 17] (Supplementary Fig. 3). Inhibition of Pim1 activity during 3F + IL6 reprogramming resulted in a significant reduction in Nanog[+] colonies (Fig. 5b), establishing a functional role for Pim1 downstream of IL6 in enhancing iPS reprogramming frequency. Pharmacological inhibition of Pim1 in 4F + IL6 reprogramming (where c-Myc levels are in excess) reduced the IL6-mediated 2-fold increase in iPS colony formation back to 4F-only levels (Fig. 5c). 4F reprogramming in the presence of Pim1 inhibitors also reduced colony formation. These results establish Pim1 as a downstream target of IL6 that augments iPS generation and also plays an endogenous role in reprogramming.

In order to confirm that the induction of *c-Myc* and *Pim1* was indeed attributable to IL6, we performed loss of function experiments in MEFs using shRNAs targeting the Il6 receptor (Supplementary Fig. 4). Knockdown of *Il6r* in MEFs by 4 distinct shRNAs blocked IL6-mediated phosphorylation of Stat3 (Fig. 5d). Moreover, loss of Il6r function resulted in a decreased induction of the Il6-gp130 target genes *c-Myc*, *Pim1*, and *Mcl1* (Fig. 5e), establishing the specificity of the shRNAs.

To assess whether Pim1 could enhance 4F reprogramming, we overexpressed Pim1 in MEFs, confirmed at the protein and mRNA level (Fig. 5f, g). Pim1 overexpression led to an increase in 4F iPS colony generation demonstrating that Pim1 can substitute for exogenous IL6 during the reprogramming process (Fig. 5h). It has been recently reported that the TLR3-NFκB innate immunity pathway increases the efficiency of reprogramming[18], and that Pim1 can activate NFκB[19]. We investigated whether exogenous IL6 could induce activation of NFκB, however, we saw no further induction of p-NFκB in MEFs upon IL6 stimulation, suggesting that IL6-Pim1 signaling may be acting via an alternate mechanism (Fig. 5i). Together these results demonstrate that IL6 acts early to enhance reprogramming and that this effect is mediated by Pim1 in a manner distinct from that of LIF (Fig. 5j).

In summary, we demonstrate here that heterokaryon global RNA profiling can reveal previously unrecognized genes and pathways that can be translated to iPS generation and that these reprogramming mechanisms share common regulators. This contrasts with several reports suggesting that the reprogramming of cells towards pluripotency by different approaches is likely to entail distinct and unrelated mechanisms in which oocytes and heterokaryons are thought to similarly reprogram in the absence of cell division, unlike iPS[20-22].

Notably, heterokaryons can reveal regulators that are transiently expressed. These regulators would typically be missed, as they are not highly expressed in either parental cell type or end-stage pluripotent cells (ES or iPS). Although heterokaryons differ from iPS in many

ways, they have noteworthy advantages over nuclear transfer (higher throughput) or iPS (more rapid and efficient), for elucidating molecules mediating reprogramming towards pluripotency. We first showed this for a candidate gene with a role early in DNA demethylation, the deaminase AID[3,23] and now show a transient early role for IL6. The data presented here demonstrate that candidates identified in heterokaryons can be successfully translated to iPS.

Our data provide the first evidence that in reprogramming to iPS, IL6 can functionally replace c-Myc, an oncogene found in most human cancers[24]. The demonstration that IL6 can augment reprogramming in the presence of the 4F implies that the effects mediated by IL6 are not solely due to the induction of c-Myc alone. IL6-mediated induction of the serine threonine kinase Pim1 accounts, at least in part, for the increased efficiency of iPS generation. Notably, like the action of IL6, the induction of c-Myc and Pim1 are transient. A corollary to our finding is the reported stage-specific role of IL6 signaling in regulating survival and senescence in lymphomagenesis[25]. Others have shown that c-Myc promotes both reprogramming and apoptosis during iPS generation[26]. Pim1 may counteract the apoptotic effects of excess c-Myc by phosphorylating and inactivating the mitochondrial pro-apoptotic protein BAD[27]. As IL6 signaling has pleiotropic effects, it is likely that other downstream effectors (in addition to Pim1, Stat3, Mcl1, and c-Myc) play a contributing role.

As in development, our findings highlight that stage-specific short-term responses to cytokines can play a major role in promoting cellular reprogramming. Exogenous secreted factors such as IL6 are involved in reprogramming to pluripotency during embryogenesis, initiated by the fusion between spermatozoa and oocytes (the quintessential fusion reprogramming scenario). Notably, IL6 also plays a role in the peri-implantation environment post-fusion.[28] Others have used heterokaryons, however, no attempts were made to translate the findings to iPS or reprogramming in general[29], even when bi-species transcriptome profiling was performed[30]. We show here that RNA-seq expands the use of heterokaryons as a discovery tool, enabling unprecedented molecular analysis of reprogramming leading to the identification and validation of unanticipated regulators.

A search for additional early regulators of iPS generation is now possible, including both facilitators of reprogramming and factors that impede the process and constitute 'barriers to reprogramming' such as those that maintain the somatic cell phenotype[31-33]. Indeed, heterokaryons are particularly well suited to discerning molecular regulators that act at the onset of reprogramming, both in a positive and negative manner, including non-coding RNA species, such as miRNAs[34] which could enhance the efficiency of the reprogramming process. The heterokaryon approach should have broad applications for gene discovery and understanding the mechanisms underlying reprogramming, including directed differentiation[1,2,31,35,36]. Biological ligands, like IL6, which induce endogenous signaling pathways are particularly advantageous as they can be added transiently to the medium, overcoming safety issues that currently plague genetic manipulations and the stable integration of genes, such as c-Myc[37]. Such studies will advance our knowledge of cellular reprogramming and improve the safety and efficacy of iPS or other reprogrammed cell types and their differentiated derivatives for use in regenerative medicine.

Supplementary Material

Refer to Web version on PubMed Central for supplementary material.

Acknowledgments

References

1. Vierbuchen T, Wernig M. Molecular roadblocks for cellular reprogramming. Molecular cell. 2012; 47:827–838.10.1016/j.molcel.2012.09.008 [PubMed: 23020854]

2. Yamanaka S, Blau HM. Nuclear reprogramming to a pluripotent state by three approaches. Nature. 2010; 465:704–712.10.1038/nature09229 [PubMed: 20535199]

3. Bhutani N, et al. Reprogramming towards pluripotency requires AID-dependent DNA demethylation. Nature. 2010; 463:1042–1047.10.1038/nature08752 [PubMed: 20027182]

4. Mortazavi A, Williams BA, McCue K, Schaeffer L, Wold B. Mapping and quantifying mammalian transcriptomes by RNA-Seq. Nature methods. 2008; 5:621–628.10.1038/nmeth.1226 [PubMed: 18516045]

5. Tarazona S, Garcia-Alcalde F, Dopazo J, Ferrer A, Conesa A. Differential expression in RNA-seq: a matter of depth. Genome research. 2011; 21:2213–2223.10.1101/gr.124321.111 [PubMed: 21903743]

6. Thomas PD, et al. PANTHER: a browsable database of gene products organized by biological function, using curated protein family and subfamily classification. Nucleic acids research. 2003; 31:334–341. [PubMed: 12520017]

7. Hirano T, Ishihara K, Hibi M. Roles of STAT3 in mediating the cell growth, differentiation and survival signals relayed through the IL-6 family of cytokine receptors. Oncogene. 2000; 19:2548–2556.10.1038/sj.onc.1203551 [PubMed: 10851053]

8. Heinrich PC, et al. Principles of interleukin (IL)-6-type cytokine signalling and its regulation. The Biochemical journal. 2003; 374:1–20.10.1042/BJ20030407 [PubMed: 12773095]

9. Puthier D, Bataille R, Amiot M. IL-6 up-regulates mcl-1 in human myeloma cells through JAK/STAT rather than ras/MAP kinase pathway. European journal of immunology. 1999; 29:3945–3950. [PubMed: 10602002]

10. Assou S, et al. A meta-analysis of human embryonic stem cells transcriptome integrated into a web-based expression atlas. Stem Cells. 2007; 25:961–973.10.1634/stemcells.2006-0352 [PubMed: 17204602]

11. Bhattacharya B, et al. Gene expression in human embryonic stem cell lines: unique molecular signature. Blood. 2004; 103:2956–2964.10.1182/blood-2003-09-3314 [PubMed: 15070671]

12. Yang J, Gao C, Chai L, Ma Y. A novel SALL4/OCT4 transcriptional feedback network for pluripotency of embryonic stem cells. PLoS One. 2010; 5:e10766.10.1371/journal.pone.0010766 [PubMed: 20505821]

13. Sridharan R, et al. Role of the murine reprogramming factors in the induction of pluripotency. Cell. 2009; 136:364–377.10.1016/j.cell.2009.01.001 [PubMed: 19167336]

14. Buganim Y, et al. Single-Cell Expression Analyses during Cellular Reprogramming Reveal an Early Stochastic and a Late Hierarchic Phase. Cell. 2012; 150:1209–1222.10.1016/j.cell.2012.08.023 [PubMed: 22980981]

15. Takahashi K, Yamanaka S. Induction of pluripotent stem cells from mouse embryonic and adult fibroblast cultures by defined factors. Cell. 2006; 126:663–676.10.1016/j.cell.2006.07.024 [PubMed: 16904174]

16. Cheney IW, et al. Identification and structure-activity relationships of substituted pyridones as inhibitors of Pim-1 kinase. Bioorganic & medicinal chemistry letters. 2007; 17:1679–1683.10.1016/j.bmcl.2006.12.086 [PubMed: 17251021]

17. Pierce AC, Jacobs M, Stuver-Moody C. Docking study yields four novel inhibitors of the protooncogene Pim-1 kinase. Journal of medicinal chemistry. 2008; 51:1972–1975.10.1021/jm701248t [PubMed: 18290603]

18. Lee J, et al. Activation of innate immunity is required for efficient nuclear reprogramming. Cell. 2012; 151:547–558.10.1016/j.cell.2012.09.034 [PubMed: 23101625]

19. Nihira K, et al. Pim-1 controls NF-kappaB signalling by stabilizing RelA/p65. Cell death and differentiation. 2010; 17:689–698.10.1038/cdd.2009.174 [PubMed: 19911008]

20. Bhutani N, et al. A critical role for AID in the initiation of reprogramming to induced pluripotent stem cells. FASEB J. 2013; 27:1107–1113.10.1096/fj.12-222125 [PubMed: 23212122]

21. Byrne JA, et al. Producing primate embryonic stem cells by somatic cell nuclear transfer. Nature. 2007; 450:497–502.10.1038/nature06357 [PubMed: 18004281]

22. Hanna J, et al. Direct cell reprogramming is a stochastic process amenable to acceleration. Nature. 2009; 462:595–601.10.1038/nature08592 [PubMed: 19898493]

23. Pasque V, Jullien J, Miyamoto K, Halley-Stott RP, Gurdon JB. Epigenetic factors influencing resistance to nuclear reprogramming. Trends Genet. 2011; 27:516–525.10.1016/j.tig.2011.08.002 [PubMed: 21940062]

24. Lin CY, et al. Transcriptional amplification in tumor cells with elevated c-Myc. Cell. 2012; 151:56–67.10.1016/j.cell.2012.08.026 [PubMed: 23021215]

25. Gilbert LA, Hemann MT. Context-specific roles for paracrine IL-6 in lymphomagenesis. Genes & development. 2012; 26:1758–1768.10.1101/gad.197590.112 [PubMed: 22855834]

26. Soufi A, Donahue G, Zaret KS. Facilitators and impediments of the pluripotency reprogramming factors' initial engagement with the genome. Cell. 2012; 151:994–1004.10.1016/j.cell.2012.09.045 [PubMed: 23159369]

27. Aho TL, et al. Pim-1 kinase promotes inactivation of the pro-apoptotic Bad protein by phosphorylating it on the Ser112 gatekeeper site. FEBS letters. 2004; 571:43–49.10.1016/j.febslet.2004.06.050 [PubMed: 15280015]

28. van Mourik MS, Macklon NS, Heijnen CJ. Embryonic implantation: cytokines, adhesion molecules, and immune cells in establishing an implantation environment. Journal of leukocyte biology. 2009; 85:4–19.10.1189/jlb.0708395 [PubMed: 18784344]

29. Tsubouchi T, et al. DNA synthesis is required for reprogramming mediated by stem cell fusion. Cell. 2013; 152:873–883.10.1016/j.cell.2013.01.012 [PubMed: 23415233]

30. Foshay KM, et al. Embryonic stem cells induce pluripotency in somatic cell fusion through biphasic reprogramming. Molecular cell. 2012; 46:159–170.10.1016/j.molcel.2012.02.013 [PubMed: 22445485]

31. Holmberg J, Perlmann T. Maintaining differentiated cellular identity. Nature reviews Genetics. 2012; 13:429–439.10.1038/nrg3209

32. Silva J, Chambers I, Pollard S, Smith A. Nanog promotes transfer of pluripotency after cell fusion. Nature. 2006; 441:997–1001. [PubMed: 16791199]

33. Pasque V, Halley-Stott RP, Gillich A, Garrett N, Gurdon JB. Epigenetic stability of repressed states involving the histone variant macroH2A revealed by nuclear transfer to Xenopus oocytes. Nucleus. 2011; 2:533–539.10.4161/nucl.2.6.17799 [PubMed: 22064467]

34. Huang XA, Lin H. The miRNA Regulation of Stem Cells. Wiley interdisciplinary reviews Membrane transport and signaling. 2012; 1:83–95.10.1002/wdev.5 [PubMed: 23024929]

35. Graf T. Historical origins of transdifferentiation and reprogramming. Cell stem cell. 2011; 9:504–516.10.1016/j.stem.2011.11.012 [PubMed: 22136926]

36. Salero E, et al. Adult human RPE can be activated into a multipotent stem cell that produces mesenchymal derivatives. Cell stem cell. 2012; 10:88–95.10.1016/j.stem.2011.11.018 [PubMed: 22226358]

37. Marson A, et al. Wnt signaling promotes reprogramming of somatic cells to pluripotency. Cell stem cell. 2008; 3:132–135.10.1016/j.stem.2008.06.019 [PubMed: 18682236]
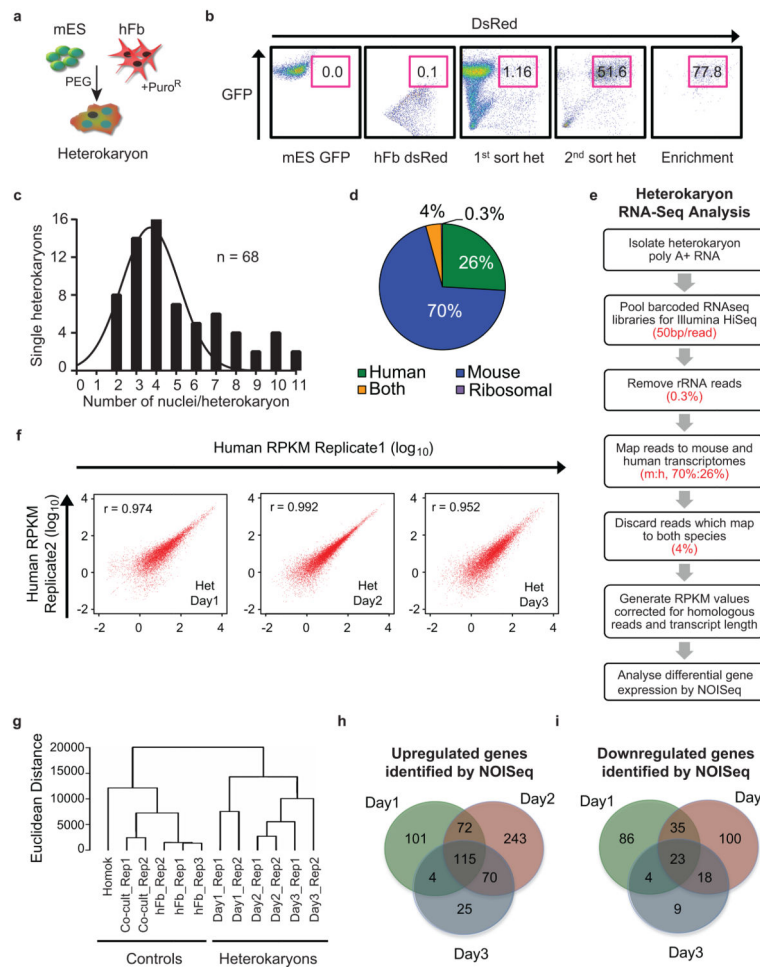
Figure 1. Heterokaryon global bi-species transcriptome analysis by RNA-Seq identifies differentially expressed genes during somatic cell reprogramming towards pluripotency

a, Scheme for heterokaryon generation. GFP mouse ES (mES) cells were co-cultured with DsRedpuro[R] primary human fibroblasts (hFb) and then fused using PEG. **b,** Heterokaryon enrichment and isolation by FACS. Representative FACS plots for heterokaryon isolation. From left to right: GFP+ mouse ES cells, DsRed+ human fibroblasts, GFP+ DsRed+ day 2 heterokaryons first sort, second sort, enrichment. **c,** Histogram of heterokaryon nuclear content (total number of nuclei per FACS sorted heterokaryon assessed by single cell microscopy, n = 68). A fitted Gaussian curve reveals an average nuclear content of 4 nuclei per heterokaryon. **d,** Average mappable read summary for heterokaryon RNA-Seq libraries. **e,** Flowchart of heterokaryon RNA-Seq analysis. **f,** Comparison of biological replicates of human gene expression during heterokaryon reprogramming for the three days. Pearson's correlation values are displayed for heterokaryon biological replicates. Replicate 1 for each day is displayed on the x-axis, and Replicate 2 for each day on the y-axis. **g,** Hierarchical cluster of RNA-Seq data for heterokaryon as well as control samples, using the Euclidean distance metric and complete linkage method. **h** and **i,** Venn diagram of significantly upregulated and downregulated gene expression in heterokaryon reprogramming compared to the homokaryon, co-culture, and unfused human fibroblasts controls. Differential gene
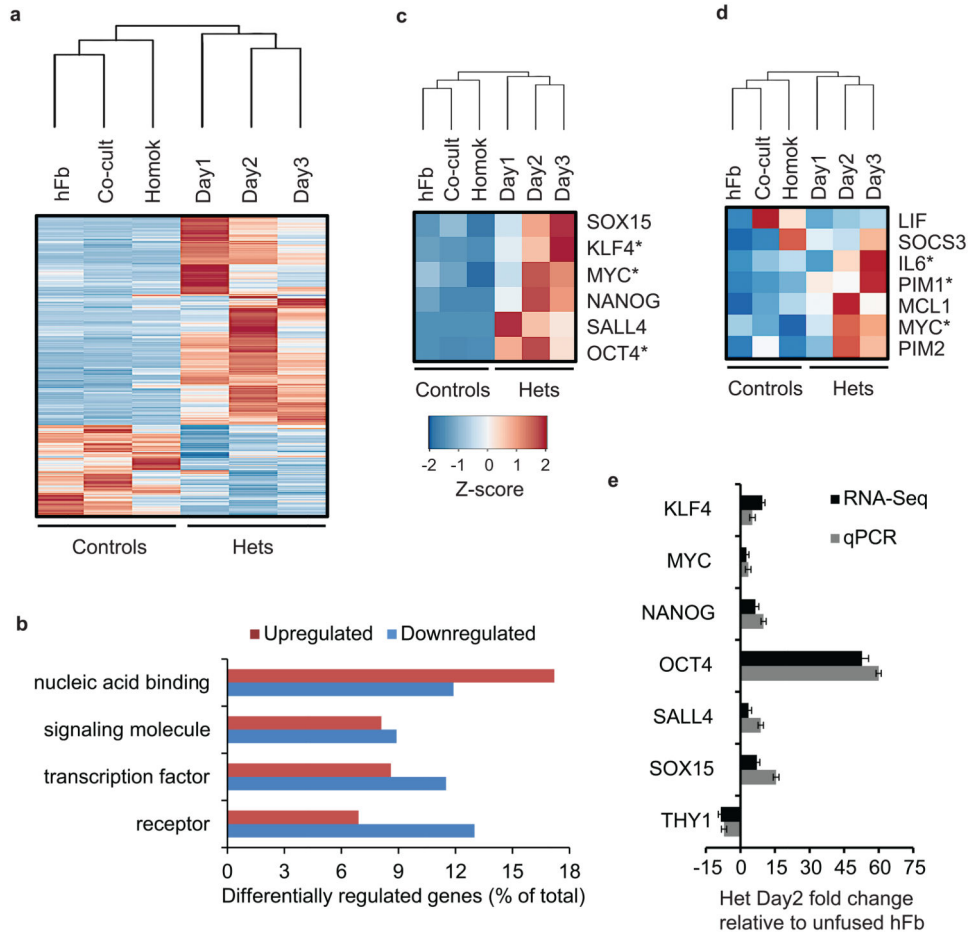
expression was identified using the NOISeq method with a cut-off probability threshold of 0.8. Source data are presented in Table SI 1.

Figure 2. Heterokaryon bi-species RNA-Seq identifies induction of GP130 signaling gene expression during somatic cell reprogramming

a, Heatmap of differentially expressed genes during heterokaryon reprogramming (day1-3 post fusion) as compared to unfused human fibroblasts, co-culture, and homokaryon (fibroblast-fibroblast fusion) controls. The gene expression (RPKM) values for each gene were normalized to the standard normal distribution to generate z-scores. The z-score color bar is shown with the minimum expression value for each gene in blue and the maximum value in red. **b,** Protein classification of the differentially expressed human genes (n=905 genes) using the PANTHER (Protein ANalysis THrough Evolutionary Relationships) classification system with default settings. Select protein classes encompassing at least 5% of the total number of upregulated genes (n=630) or downregulated genes (n=275) are shown. **c, d,** Heatmap of human pluripotency transcription factors and GP130 signaling gene pathway genes, respectively, during heterokaryon reprogramming. Normalized gene expression values were used (see above). **e,** Validation of heterokaryon RNA-Seq gene expression levels by qPCR for six human pluripotency genes and the lineage marker THY1 (Day 2 post fusion), relative to unfused human fibroblasts. Data are represented as mean ± s.d. for qPCR data (n=3) and mean with range (n=2) for RNA-Seq data.
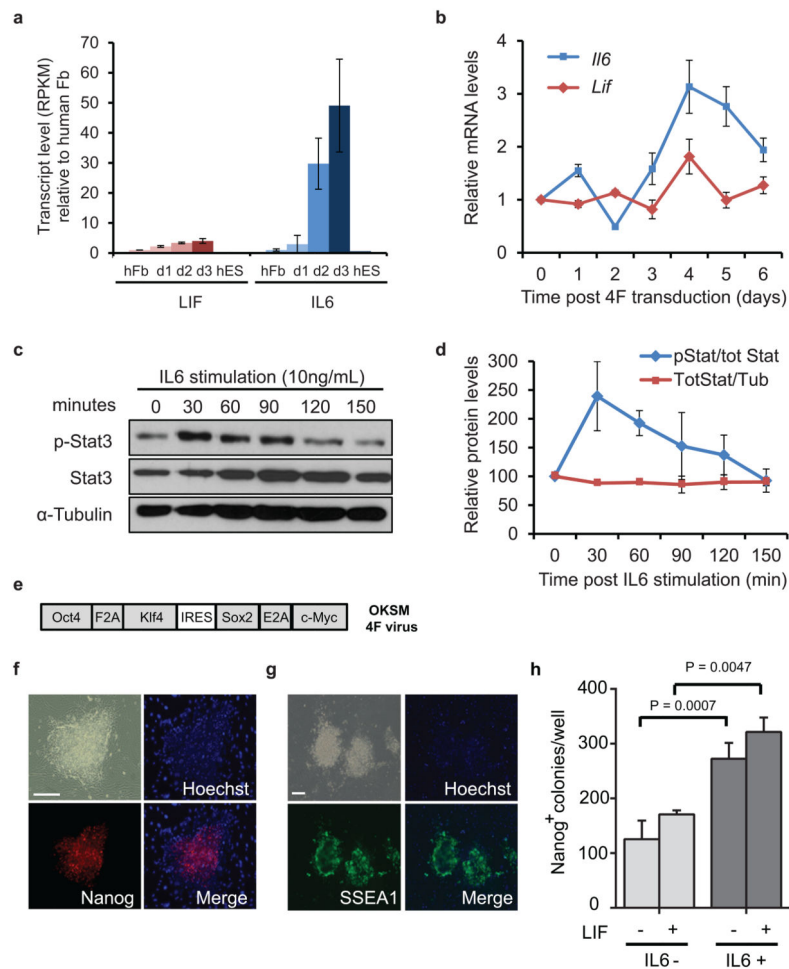
Figure 3. IL6, but not LIF, enhances 4 Factor iPS generation

a, Relative transcript levels of LIF and IL6 during heterokaryon reprogramming, normalized to unfused human fibroblasts. Data are represented as mean RPKM withrange (n=2). **b,** Relative mRNA levels for *Il6* and *Lif* gene expression during 4 Factor (4F) iPS generation in MEFs, normalized to mouse *Hprt* and mouse *Gapdh*, as determined by qPCR. Data are represented as mean ± s.e.m., n=4. **c,** Induction of pStat3 Tyr-705 in fibroblasts upon IL6 stimulation. A representative western blot over a 2.5 hour time course is shown. Full blot is shown in Supplementary Fig. 5. **d,** Quantification of pStat3 induction upon IL6 stimulation, normalized to α-Tubulin protein levels. Mean with range is shown (n=2). Maximal pStat3 is observed 30 minutes post-IL6 stimulation. **e,** Schematic of the 4Factorlentiviral vector used to generate 4F (OKSM) virus for mouse iPS induction. **f,** Phase and immunofluorescence images of a representative iPS colony stained for the mouse pluripotency marker Nanog (red) and nuclear Hoechst (blue). Scale bar = 200 μm. **g,** Representative iPS colonies, presented as in f with staining for the mouse pluripotency marker SSEA-1 (green). **h,** Nanog[+] iPS colony formation from MEFs transduced with Mock or 4F virus in the absence of additional cytokines and cultured with or without IL6 and or LIF. Data are represented as mean ± s.e.m., n=3. P values were calculated using Student's unpaired two-tailed t-test. Source data are presented in Table SI 1.
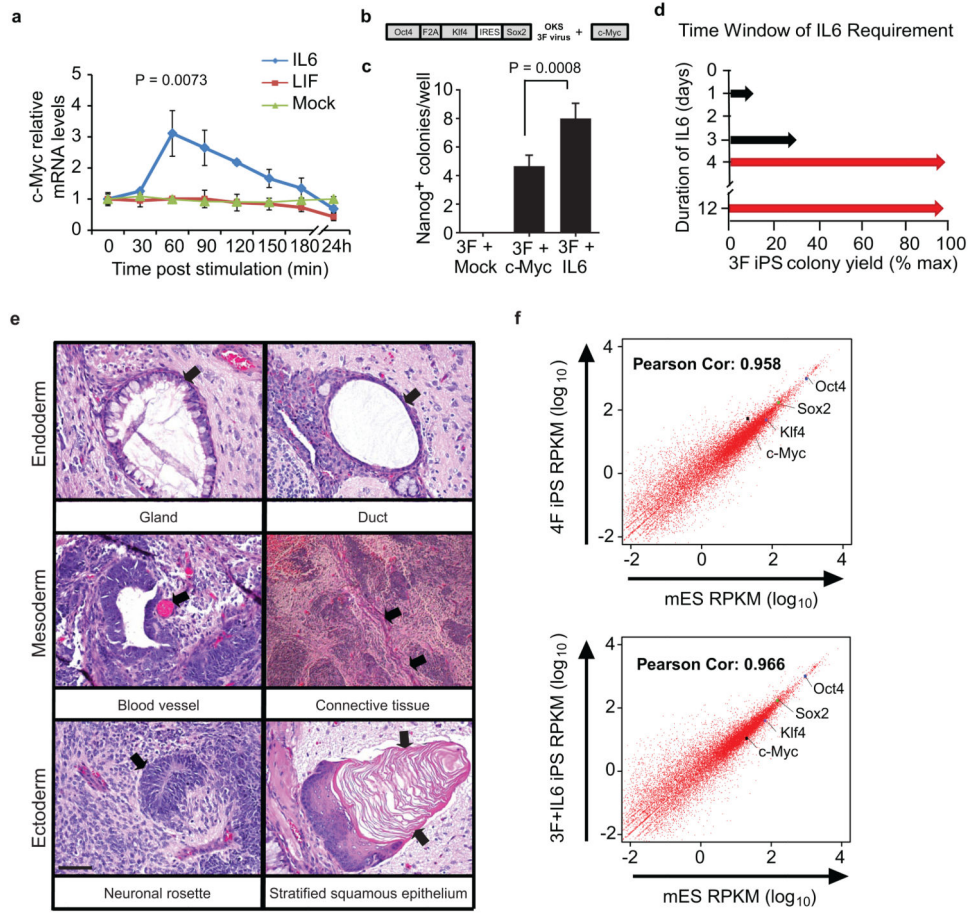
Figure 4. Transient exposure to IL6 in medium replaces viral c-Myc in reprogramming to iPS and is only required at the onset of 3F reprogramming

a, Timecourse of relative mRNA expression levels for endogenous c-Myc in MEFs after stimulation with IL6, LIF, or mock (medium change only), normalized to mouse *Actin* and t=0 min. Data are represented as mean ±s.d., n=3. P values were calculated using Student's unpaired two-tailed t-test. Source data are presented in Table SI 1. **b,** Schematic of the 3F lentiviral vector. c-Myc was restored using a second virus when indicated. **c,** Nanog+ iPS colony formation from MEFs transduced with 3F virus with or without IL6 or co-transduction with Mock or c-Myc virus. Data are represented as mean ± s.e.m., n=6. P values were calculated using Student's unpaired two-tailed t-test. Source data are presented in Table SI 1. **d,** Nanog+ iPS colony formation from MEFs upon IL6 withdrawal from the medium on the day indicated. Maximum colony yield is obtained when IL6 is added to the medium for the first four days of reprogramming. Treatment beyond day 4 did not increase iPS colony number. **e,** Teratoma histological analysis from 3F + IL6 iPS clones 1 and 4 showing contribution to all three germ layers. Magnification is 200×, scale bar = 50 μm. **f,** Comparison of global gene expression between individually generated iPS (4F and 3F+IL6) clones and mES (average of n=2 for each). The Pearson's correlation values are displayed for iPS versus mES gene expression.
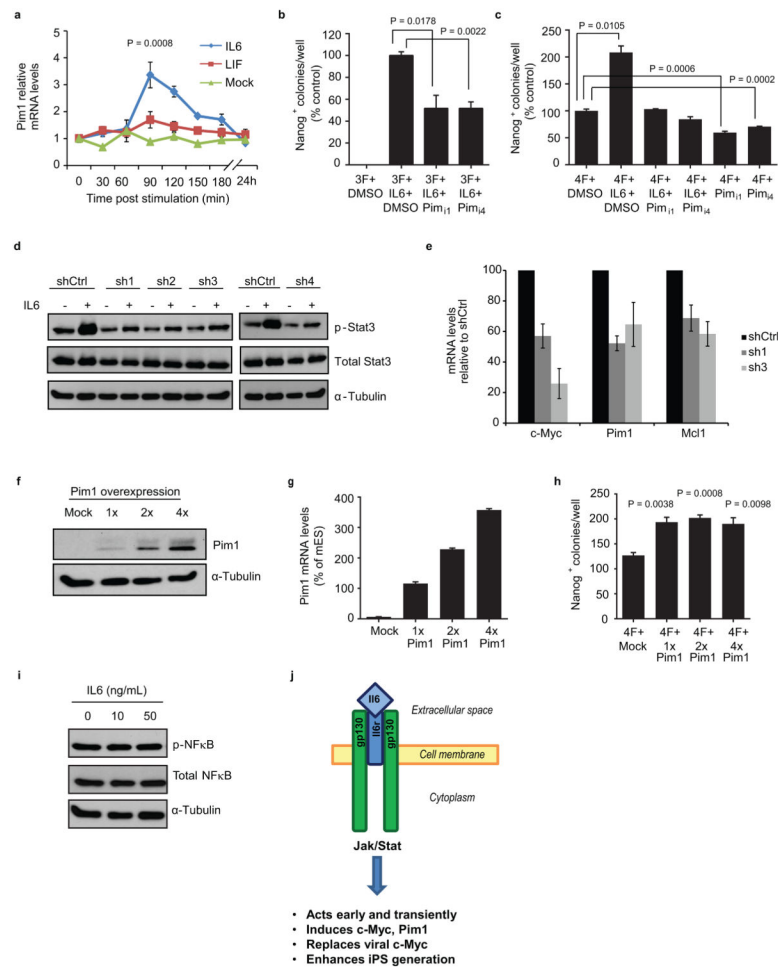
Figure 5. Pim1, a pro-survival gene, acts downstream of IL6 to enhance reprogramming to iPS
a, Timecourse of Pim1 mRNA expression levels in MEFs after stimulation with IL6, LIF, or mock (medium change only). Gene expression was normalized to *Actin* and t=0 min, as determined by qPCR (mean ±s.d., n=3). Data are presented in Table SI 1. **b,** Nanog$^+$ iPS colony formation from MEFs transduced with 3F virus with or without addition of IL6, Pim1 inhibitor or DMSO (mean ± s.e.m., n=3, shown as a percent of control). Data are presented in Table SI 1. **c,** Nanog$^+$ iPS colony formation from MEFs transduced with 4F virus, with or without IL6, Pim1 inhibitor or DMSO as indicated, shown as a percent of control (mean ± s.e.m., n=3). Data are presented in Table SI 1. **d,** Western blots of p-Stat3 induction in MEFs transduced with shRNAs against Il6r or shControl, assessed 30 minutes post stimulation with IL6 or mock. MEFs were stimulated 3 days after shRNA virus transduction. Total Stat3 levels and α-tubulin levels are shown as a reference and loading control, respectively. **e,** Mouse c-Myc, Pim1, and Mcl1 mRNA levels in MEFs transduced with shRNA virus targeting Il6r or control shRNA virus and stimulated with IL6, as assessed by qPCR. mRNA expression levels were normalized to mouse *Actin* and assessed at peak shControl levels post Il6 stimulation occurring at 60, 90, and 120min post stimulation, respectively (mean ±s.d., n=3). Data are presented in Table SI 1. **f,** Western blot for Pim1 overexpression in MEFs. **g,** Pim1 mRNA levels in MEFs transduced with Pim1

virus, as determined by qPCR, normalized to *Actin* and *Pim1* levels in mES (mean ± s.d., n=3). Data are presented in Table SI 1. **h,** Nanog[+] iPS colony formation from MEFs transduced with 4F and Pim1 virus or mock virus (mean ± s.e.m., n=3). Data are presented in Table SI 1. **i,** Western blot for p-NFκB protein levels in IL6 treated MEFs, 3 hours post-stimulation with IL6. NFκB and α-Tubulin are shown as controls. **j,** Model for early IL6-mediated enhancement of iPS generation. The yellow rectangle indicates the cell membrane containing the Gp130 and Il6 receptor. Il6 ligand is depicted as a diamond. Extracellular space and cytoplasm are indicated. P values were calculated using Student's unpaired two-tailed t-test. Full blots are shown in Supplementary Fig. 5.